



Available online at [www.sciencedirect.com](http://www.sciencedirect.com)

SCIENCE @ DIRECT®

**Precambrian  
Research**

Precambrian Research 138 (2005) 208–224

[www.elsevier.com/locate/precamres](http://www.elsevier.com/locate/precamres)

# Combined micro-Fourier transform infrared (FTIR) spectroscopy and micro-Raman spectroscopy of Proterozoic acritarchs: A new approach to Palaeobiology

Craig P. Marshall <sup>a,\*</sup>, Emmanuelle J. Javaux <sup>b</sup>,  
Andrew H. Knoll <sup>c</sup>, Malcolm R. Walter Javaux,

<sup>b</sup> *Department of Astrophysics, Geophysics and Oceanography, University of Liège,  
17 Allée du 6 Août, B5c, 4000 Liège (Sart-Tilman), Belgium*

<sup>c</sup> *Department of Organismic and Evolutionary Biology, Harvard University, 26 Oxford Street, Cambridge, MA 02138, USA*

Received 11 February 2005; received in revised form 6 May 2005; accepted 13 May 2005

---

## Abstract

Micro-scale analytical techniques permit correlation of chemistry with morphology of individual Proterozoic acritarchs (organic-walled microfossils), and thus provide new approaches for elucidating their biological affinities. A combination of micro-Fourier transform infrared (FTIR) spectroscopy and laser micro-Raman spectroscopy was used to investigate the organic structure and composition of individual acritarchs. Well preserved Neoproterozoic acritarchs from the Tanana Formation, Aus-



dinoflagellate specific biomarkers, dinosteranes and 4 $\alpha$ -methyl-24-ethylsteranes, in the pyrolysates of Early Cambrian mixed acritarch concentrates. However, even these careful analyses tell us only that biomarker-producing dinoflagellates and cyst-producing cells lived in the same environment. We know of no reports these biomarkers from older, individually analysed acritarchs.

Arouri et al. (1999) analysed two Neoproterozoic acritarchs, *Multifronsphaeridium pelorium* and the informally designated Species A, by Scanning Electron Microscopy (SEM), Transmission Electron Microscopy (TEM), micro-FTIR spectroscopy, py-GC/MS, and thermal desorption MS. The macromolecular structure of *Multifronsphaeridium pelorium* and Species A consisted of short *n*-alkylpolymethylenic chains, probably linked via ether/ester bonds, with possibly a small aromatic content. They concluded that the ultrastructural and molecular results show evidence for a phylogenetic relationship between these acritarchs and Chlorophyceae (see Versteegh and Blokker, 2004, for commentary). In a further study, Arouri et al. (2000) analysed a range of Neoproterozoic acritarchs (*Tanarium* sp., *Hocosphaeridium scaber-facium*, *Alicesphaeridium medusoidum*, *Chuarina circularis*, *Leiosphaeridia* sp., and *Tasmanites* sp.) by micro-FTIR spectroscopy, py-GC/MS, and laser Raman spectroscopy. They concluded that little chemical data was obtained by micro-FTIR spectroscopy and py-GC/MS and this was consistent with a polyaromatic biomacromolecule of high recalcitrance. In addition, they interpreted their Raman spectra to show a signal attributable to significant carbon ordering characteristic of polyaromatic structures. However, the correct interpretation of their Raman spectra is that the macromolecular network consists of low thermally matured disordered  $sp^2$  carbon. These results led the authors to the conclusion that the acritarchs are composed of a polyaromatic biopolymer indicating a genetic relationship with dinoflagellates. Such studies form a basis for our microchemical analyses of the older acritarchs that provide our earliest well characterized evidence for eukaryotic diversification.

The aims of this paper are to develop a micro-FTIR spectroscopic method tailored to micro-scale characterization of Proterozoic acritarchs, to elucidate their cyst wall biopolymer composition, and, thus, to establish their biological affinities. In this study, we

also assess the possibility of using laser Raman spectroscopy to obtain useful information pertaining to biopolymer composition of microfossils. By comparison with biomarker analyses, micro-FTIR and micro-Raman techniques have the great advantages of being applicable on a very small sample (such as one microfossil), of providing data on the chemical composition of microfossils with previously described morphology and ultrastructure, and of avoiding contamination problems. Thus, the techniques used in this study extend the approach of Arouri et al. (1999, 2000) in relating fossil

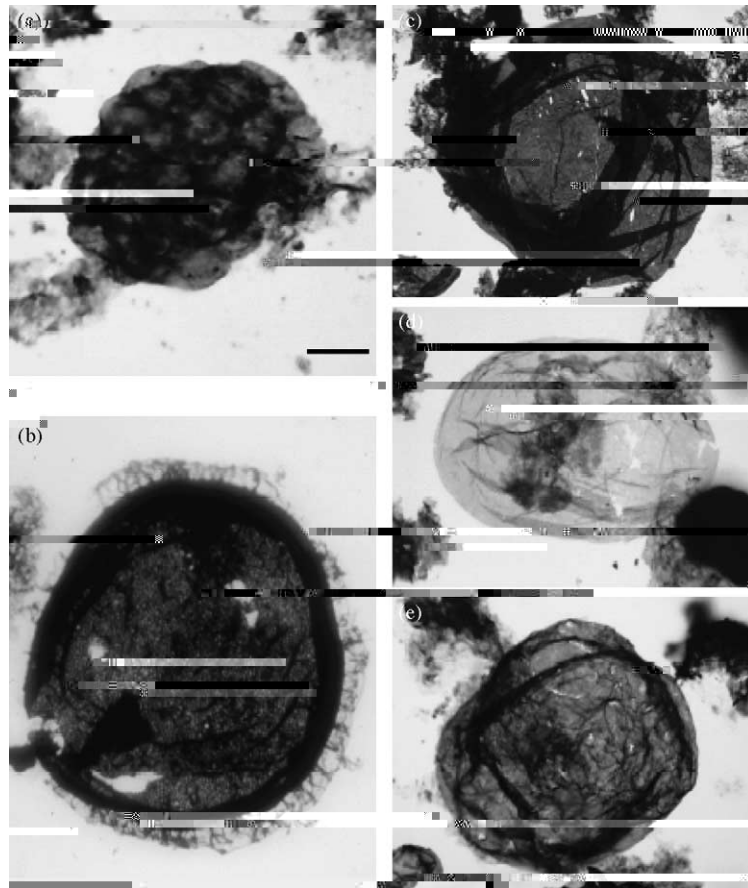


Fig. 1. Light photographs of analyzed species. (a) and (c)–(e): microfossils from the Roper Group, Australia; (b): microfossil from the Ruyang Group, China. (a) *Satka squamifera*; (b) *Shuiyousphaeridium macroreticulatum*; (c) *Leiosphaeridia jacutica*; (d) *Leiosphaeridia tenuissima*; (e) *Leiosphaeridia crassa*. Scale bar in (a) is 15  $\mu\text{m}$  for (a) and (d); 46  $\mu\text{m}$  for (b); 20  $\mu\text{m}$  for (c); 10  $\mu\text{m}$  for (e).

*conoideum* and *Leiosphaeridia* sp. (Fig. 2b, Arouri et al., 2000, p. 80).

### 2.3. Microscopy and TAI assessment

Thermal Alteration Index (TAI) observations were made using an Olympus BH2 microscope. The TAI scale of Batten (1996) was used as the standard.

### 2.4. Micro-Fourier transform infrared (FTIR) spectroscopy

Micro-analytical techniques have been applied to two or three specimens of each taxon. Micro-FTIR spectroscopic analyses were performed using a Bruker

IFS66 Fourier transform infrared spectrometer coupled to a Bruker microscope accessory housing a dedicated liquid nitrogen cooled (77 K), narrow-band mercury cadmium telluride detector. The microscope was fitted with an IR/visible Cassegrainian 15 $\times$  objective (numerical aperture = 0.4). Acritarch samples were placed on potassium bromide slides. Interferograms were acquired in the transmission mode within the range 4000–900  $\text{cm}^{-1}$ .

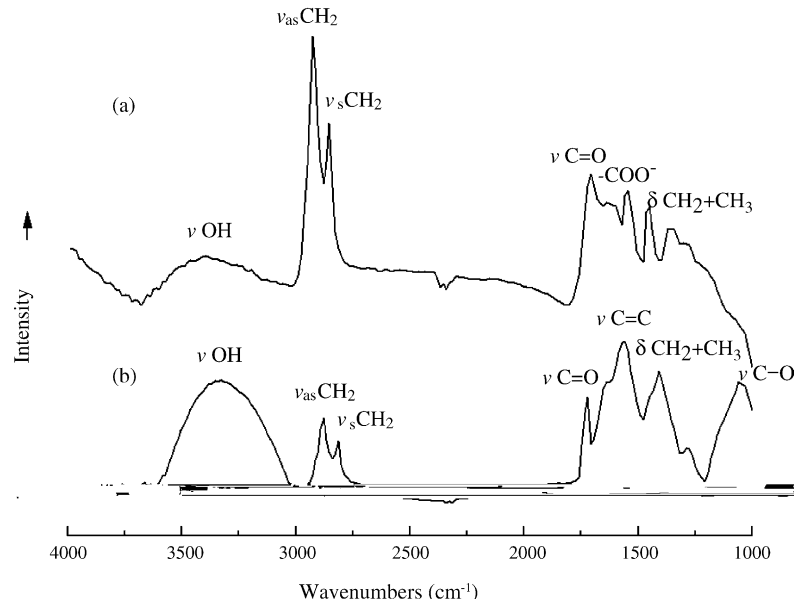


Fig. 2. Representative micro-FTIR spectra of Neoproterozoic acritarchs: (a) *Tanarium 'conoideum* and (b) *Leiosphaeridia* sp. Refer to Table 2 for band assignments.

gram (GRAM/32 software). The aliphatic region was baseline-linearized using an interactive procedure of the program by connecting the left and right points of

signal-to-noise ratio of the spectra. The scan ranges were 1000–1800  $\text{cm}^{-1}$  in the carbon first-order region. Acritarchs were deposited on clean aluminum microscope slides and irradiated with the laser to obtain spectra.

### 3. Results

#### 3.1. TAI assessments

Table 1 lists the acritarch genera studied here, along with drill hole information, stratigraphic location, and TAI, as determined from the scale of Batten (1996). Most palynomorphs, including acritarchs, show sequential colour and structural changes in response to increasing depth of burial related to the thermal history of the enclosing sediment. The acritarchs used in this study show sequential colour changes from yellow to orange–brown (Table 1) corresponding to a TAI range from 1/2 to 4, approximately equivalent to a vitrinite reflectance of 0.2–0.75% (Senftle and Landis, 1991; Traverse, 1988). These thermal maturity indicators show that the organic matter in the acritarchs ranges from immature to oil window (mature). The low thermal maturity of these acritarchs makes them ideally suited for microchemical analysis. Nevertheless, while morphologically well preserved, these acritarchs have undergone some degree of diagenesis, potentially removing more labile components and

leaving the more robust and selectively preserved macromolecular structures. Therefore, it is relevant to compare these selectively preserved biopolymers with non-hydrolyzable biomacromolecules isolated from extant microorganisms.

Several criteria have been proposed to differentiate eukaryotic from prokaryotic fossil cells (Javaux et al., 2003 and references therein). Previous TEM and SEM studies (Javaux et al., 2001, 2003, 2004a,b) indicate that some Mesoproterozoic acritarchs display complex surface ornaments, wall structures and/or multi-layered wall ultrastructures unknown in prokaryotic cells but similar in general to those of extant protists. The chemical composition of the acritarch cyst might also reveal eukaryotic attributes, but in addition, biopolymer composition may elucidate the finer-scale systematic affinities of microfossils, when morphology and ultrastructure are inadequate for the task.

#### 3.2. General IR Characteristics of the Acritarchs

Typical peak assignments and intensities observed by micro-FTIR spectroscopy for each acritarch sample are given in Table 2.

The one acritarch that contains abundant aliphatic structures, as indicated by the very strong aliphatic C–H<sub>x</sub> bands (strong methylene stretching and bending band at 2930–2860 and 1450  $\text{cm}^{-1}$ , respectively) is *Tanarium conoideum* from the Neoproterozoic Tanana Formation (Fig. 2a). The spectrum shows absorptions

Table 1

Acritarch genera studied here, along with their drill hole information, stratigraphic location, and TAI as determined from the scale of Batten (1996)

Acritarch	Stratigraphy	Drill hole	Acritarch colour	TAI	Degree of maturation	Equilivant $R_0$
-----------	--------------	------------	------------------	-----	----------------------	------------------

Table 2  
Typical peak assignments and intensities observed by micro-FTIR spectroscopy for each acritarch sample

Wavenumber (cm <sup>-1</sup> )	Assignment	<i>Tanarium conoideum</i>	<i>Leiosphaeridia</i> sp.	<i>Leiosphaeridia tenuissima</i>	<i>Leiosphaeridia jacutica</i>	<i>Leiosphaeridia crassa</i>	<i>Shuiyousphaeridium macroreticulatum</i>	<i>Satka squamifera</i>
3350–3450	O–H stretch	W	S	M	M	M	M	M
2920	Antisymmetric methylene CH <sub>2</sub> stretch	S	M	W	W	W	W	W
2850	Symmetric methylene CH <sub>2</sub> stretch	S	M	W	W	W	W	W
1710	Carbonyl C=O stretch	W	S	Shoulder	Shoulder	Shoulder	W	W
1600	C=C aromatic ring stretch	Np	S	S	S	S	S	S
1532	Aliphatic COOH	Np	Np	Shoulder	Shoulder	Shoulder	Shoulder	S
1450	Methylene CH <sub>2</sub> bend	S	S	Np	Np	Np	Np	W
1345	Terminal methyl CH <sub>3</sub>	Np	Np	S	S	S	S	S
1275	C–O stretching aliphatic ethers	Np	S	W	W	W	W	W
900–700	=C–H aromatic deformation	Np	Np	W	W	W	W	W

W, weak; M, moderate; S, strong; and Np, not present.

centered at: a low broad absorption at  $3468\text{ cm}^{-1}$  assigned to alcoholic OH, phenolic OH, and/or carboxylic OH; strong narrow aliphatic absorptions centered at  $2920$  and  $2850\text{ cm}^{-1}$  assigned to asymmetric stretching vibrations from  $\text{CH}_2$  and symmetric stretching vibrations from  $\text{CH}_2$  methylene groups, respectively; a weak absorption centered at  $1710\text{ cm}^{-1}$  assigned to the vibration of carbonyl  $\text{C}=\text{O}$ ; moderate absorptions of deformation bending of  $\text{CH}_2$  and  $\text{CH}_3$  centered at  $1450\text{ cm}^{-1}$ ; and minor absorptions of ether ( $\text{C}-\text{O}$ ) bonding between  $1200$  and  $1000\text{ cm}^{-1}$ . A strong methylene stretching and bending band ( $2930$ – $2860$  and  $1450\text{ cm}^{-1}$ , respectively) and a weak methyl band indicate a long-chain linear aliphatic structure. The observation of abundant aliphatic structures of cell wall organic material for this acritarch is consistent with that of algaenans isolated from green microalgae (for example, Gelin et al., 1999 and references therein). This representative spectrum acquired from *Tanarium conoideum* is in disagreement with that spectrum obtained from the *Tanarium conoideum* acritarch in Fig. 4 of Arouri et al. (2000). The spectrum in Fig. 4 of Arouri et al. (2000) shows little to no vibration of organic material, and in addition the spectra are heavily dominated by water and carbon dioxide, suggesting instrument or sample preparation problems.

The FTIR spectrum obtained from analyses of *Leiosphaeridia* sp., differs substantially from that of *Tanarium conoideum*. Spectra obtained from *Tanarium conoideum* show a greater aliphatic character than the *Leiosphaeridia* sp. even though these microfossils are isolated from the same core interval. This clearly shows that the inferred differences in biopolymer composition are controlled by the biological source rather than thermal maturity. A representative micro-FTIR spectrum obtained from a single *Leiosphaeridia* sp. acritarch from the Tanana Formation is shown in Fig. 2b. The spectrum shows absorptions centered at: a strong broad absorption at  $3468\text{ cm}^{-1}$  assigned to alcoholic OH, phenolic OH, and/or carboxylic OH; strong narrow aliphatic absorptions centered at  $2920$  and  $2850\text{ cm}^{-1}$  assigned to asymmetric stretching vibrations from  $\text{CH}_2$  and symmetric stretching vibrations from  $\text{CH}_2$  methylene groups, respectively; a moderate absorption centered at  $1710\text{ cm}^{-1}$  assigned to the vibration of carbonyl  $\text{C}=\text{O}$ ; a strong absorption of olefinic  $\text{C}=\text{C}$  centered at  $1600\text{ cm}^{-1}$ ; moderate absorptions of deformation bending of  $\text{CH}_2$  and

$\text{CH}_3$  centered at  $1450\text{ cm}^{-1}$ ; and a strong broad absorption of aliphatic ether ( $\text{C}-\text{O}$ ) bonding centered at  $1090\text{ cm}^{-1}$ . Closer inspection of the line-shape and relative magnitude of the aliphatic  $\text{C}-\text{H}_x$  stretching region,  $3000$ – $2700\text{ cm}^{-1}$ , shows a slight shoulder at  $2960\text{ cm}^{-1}$  (asy  $\text{C}-\text{H}$  str of methyl groups) and a low width of the band centered at  $2920\text{ cm}^{-1}$ , which indicates a substantial contribution of polymethylenic chains with a low degree of branching.

Representative micro-FTIR spectra acquired for three leiospheres in the Mesoproterozoic Roper assemblage (*Leiosphaeridia crassa*, *L. jacutica*, *L. tenuissima*), are similar and for brevity the spectra acquired from *L. jacutica* and *Satka squamifera* are shown in Fig. 3a and b, respectively. The spectra show absorptions centered at: a strong broad absorption at

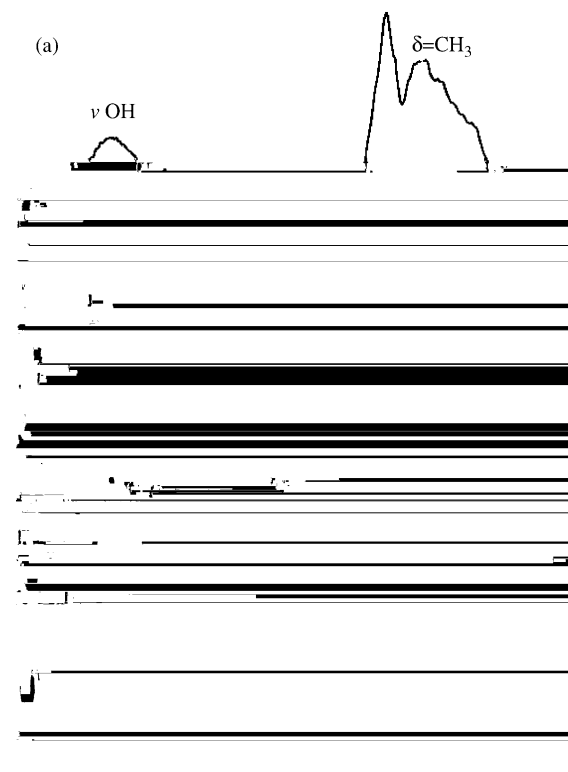
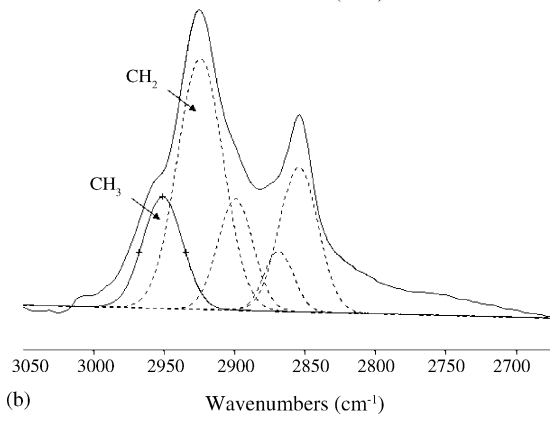
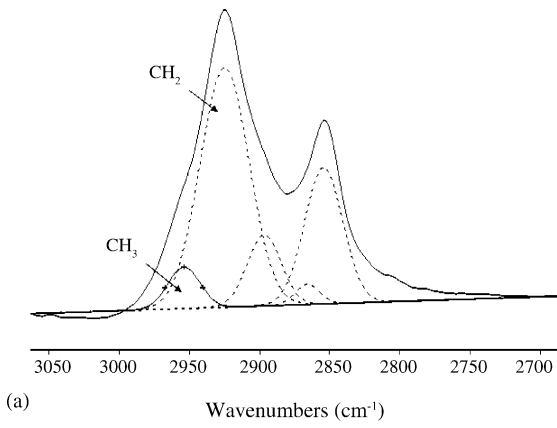


Fig. 3. Representative micro-FTIR spectra of Mesoproterozoic acritarchs: (a) *Leiosphaeridia jacutica*; (b) *Satka squamifera*; and (c) *Shuiyousphaeridium macroreticulatum*. Refer to Table 2 for band assignments.



3379 cm<sup>-1</sup> assigned to alcoholic OH, phenolic OH,  
and/or carboxylic OH; medium aliphatic absorptions



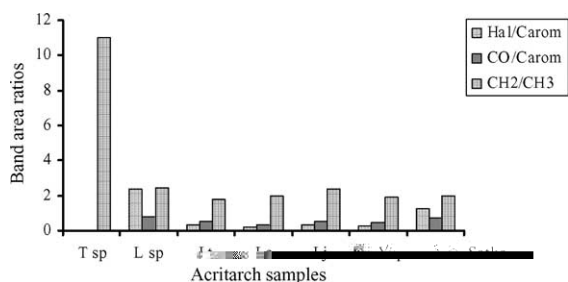


Fig. 5. Plot of peak intensity ratios determined from FTIR spectra of aliphatic C–H ( $2930\text{--}2850\text{ cm}^{-1}$ )/aromatic C=C ( $1600\text{ cm}^{-1}$ ) ( $H_{al}/C_{ar}$ ), carbonyl CO groups ( $1710\text{ cm}^{-1}$ )/aromatic carbon ( $1600\text{ cm}^{-1}$ ) content of the acritarchs ( $CO/C_{ar}$ ), and the methylene ( $CH_2$ )/methyl ( $CH_3$ ).

the Tanana Formation shows a different biopolymer composition which still consists of linear long chain aliphatic hydrocarbons but has a degree of branching, aliphatic ether bonds, and some olefinic hydrocarbon. *Leiosphaeridia crassa*, *L. jacutica*, *L. tenuissima*, and *Shuiyousphaeridium macroreticulatum* from the Mesoproterozoic Roper and Ruyang groups have similar biopolymer compositions, predominantly aromatic with a low content of highly branched aliphatic chains. The biopolymer composition of *Satka squamifera* biopolymer is notably different, however, in that it contains a greater amount of aliphatic hydrocarbon and carboxyl groups, and the degree of branching is less than the other biopolymer compositions of Roper Group acritarchs.

### 3.5. Laser micro-Raman spectroscopy

Raman spectra of carbonaceous materials can be divided into two spectral components: the first-order and the second-order spectrum (Vidano and Fischbach, 1978; Nemanich and Solin, 1979). The band assignments will be briefly discussed below for the first-order region; more extensive reviews of various interpretations for the Raman spectra of carbonaceous materials, refer to Dresselhaus and Dresselhaus (1982) and Ferrari and Robertson (2000). The samples analysed in this study do not show spectral features in the second-order region and therefore this region will not be discussed.

The first-order Raman spectrum of hexagonal graphite consists of a single, strong band at  $1582\text{ cm}^{-1}$ ; this is designated the G band due to the vibrational mode of  $E_{2g2}$  symmetry (assigned to in-plane stretch-

ing motion of pairs of carbon  $sp^2$  atoms). In addition to this strong band there is a weak band at  $42\text{ cm}^{-1}$  due to the  $E_{2g1}$  vibrational mode, which is not resolvable from Rayleigh scattering. For disordered  $sp^2$  carbons, additional bands appear at  $1150$ ,  $\sim 1350$ ,  $\sim 1500$ , and  $1620\text{ cm}^{-1}$ . The band at  $1150\text{ cm}^{-1}$  occurs in very disordered carbonaceous material (1956).



and can be preserved as ultralaminae (Hatcher et al., 1983; Largeau et al., 1986; Goth et al., 1988; Tegelaar et al., 1989). The wall of the fossil prasinophyte *Tasmanites* may also contain algaenan (see discussion in Versteegh and Blokker, 2004).

In contrast, few studies have been performed on the chemistry of vegetative cell or resting cyst walls from other microorganisms. Prokaryotic biopolymers called cyanobacteran or bacteran have been shown to be artifacts of the isolation procedure (Allard et al., 1997). On the basis of distinct physical properties, biopolymer in dinoflagellate resting cyst walls was given the name dinosporin (to distinguish it from sporopollenin; Sarjeant, 1986). Recently, studies by Kokinos (1994) and Kokinos et al. (1998) of the cysts of the marine dinoflagellate *Lingulodinium polyedrum* revealed it to be made up of a highly resistant aromatic macromolecular substance different from algaenans. More recently, studies of the cyst wall of certain acritarchs from Australian Ediacaran palynofloras suggested that these fossils also contain dinosporin (Arouri et al., 2000), providing chemical evidence of a link between Neoproterozoic acritarchs and dinoflagellates. However, caution must be applied to this interpretation due to the nature of the reported vibrational spectroscopic data. Distinct FTIR signals detected in our study of *Tanarium conoideum* and *Leiosphaeridia* sp. acritarchs contrast with the essentially featureless FTIR spectra recorded for the same samples shown by Arouri et al. (2000). These authors attribute the featureless nature of their IR spectra to the graphitic nature of the acritarch samples. However, the IR spectrum of graphite does not resemble that acquired from their acritarch samples, nor do their Raman spectra resemble spectra obtained from graphite or graphitic-like

compositions of micro-eukaryotes such as euglenids, kinetoplastids, heterokonts, ciliates, red algae, and fungi, indicating a clear need for expanded microchemical and ultrastructural research on living microorganisms.

The three species of leiopheres from the Roper Group show distinct multilayered wall ultrastructures (Javaux et al., 2004a), but similar chemical composition, underscoring the importance of combined morphological, ultrastructural, and microchemical analyses. Conversely, acritarchs with simple morphologies (leiosphaerids), and with very complex ornamentations, wall structure and ultrastructure (*Shuiyousphaeridium macroreticulatum*), have a similar biopolymer composition. The morphology and chemical composition of *Shuiyousphaeridium macroreticulatum* are compatible with a dinoflagellate affinity but could also occur in other microorganisms (Javaux and Marshall, submitted). *Shuiyousphaeridium macroreticulatum* does not show evidence of a trilaminar structure (TLS) in its wall (Javaux et al., 2004a), nor the presence of the aliphatic biopolymer algaenan (this paper); two characteristics of several extant chlorococcalean and eustigmatophycean green algae. However, not all green algae show these features, so their absence in *Shuiyousphaeridium macroreticulatum* does not preclude a green algal affinity for this taxon. Butterfield (2005) suggested a possible fungal affinity for *Shuiyousphaeridium macroreticulatum* based on general morphological similarities with fungal ascocarp (although underlining that this is certainly not established), or at least a multicellular organism not necessarily photoautotrophic. Combined analysis of the fine structure with SEM and TEM show that this acanthomorph acritarch has a reticulate wall of imbricated, beveled polygonal plates (Javaux et al., 2004a), and not of thickened, polygonal cells as might be suggested on the base of light microscopy alone (Butterfield, 2005). This species also shows medial split excystment structures, suggesting a cyst-like morphology, but whether it was a metabolically inert stage of a unicellular or multicellular organism, or whether it had a phototrophic or heterotrophic metabolism, is unknown (Butterfield, 2005; Javaux and Marshall, submitted). On the other hand, *Satka squamifera* displays a morphology (a pack of cells in an envelope) that could be prokaryotic or eukaryotic, and has a slightly different biopolymer composition, as mentioned

above. None of the early Mesoproterozoic acritarch walls studied here are composed of algaenan. In summary, then, the biological affinities of Mesoproterozoic acritarchs analyzed to date remain unknown. They could represent stem eukaryotes or extinct crown group clades that produced biopolymers distinct from those of extant groups, or they might belong to extant taxa that synthesize as yet uncharacterized biopolymers.

Our data demonstrate that Raman spectroscopy alone cannot establish the biological affinities of acritarchs; it can provide complementary information on molecular structure when combined with FTIR spectroscopy. The major limitation of Raman spectroscopy in this study resides in only showing the spectral features indicative of disordered  $sp^2$  hybridised carbon bonded to carbon. Typical Raman spectra of ancient kerogens or even of much younger coals (for example, Beny-Bassez and Rouzaud, 1985; Jehlicka et al., 1997; Spotl et al., 1998; Keleman and Fang, 2001) show only  $sp^2$  hybridised carbon bonded to carbon that have undergone degradation in which functional groups are not preserved. However, in more recent bio-

high thermal alteration, but rather reflects an indigenous polyaromatic macromolecule. This is suggested by the more aliphatic composition of the more thermally mature *Satka squamifera* relative to the Mesoproterozoic leiospheres, characterized by a more aromatic biopolymer.

Raman spectroscopy does not provide useful information about the biopolymer composition of Proterozoic acritarchs but rather elucidates the structure and thermal alteration of constituent carbonaceous material. This should be borne in mind when applying micro-Raman spectroscopy to Archean and Proterozoic microfossils.

More research is needed to characterize the chemical and morphological signatures of the full range of recent prokaryotes and protists that produce fossilizable cells. Indeed, a great limitation in detecting the biological affinities of microfossils is our currently limited knowledge of the morphology and chemical composition of decay-resistant cellular structures produced by various living microorganisms. Our ongoing research includes the determination and characterization of resistant biopolymers in a range of living prokaryotes, protists and fungi by combined microscopy and micro-FTIR spectroscopy.

### Acknowledgments

We thank Kath Grey for providing Observatory Hill samples and Shuhai Xiao for the Ruyang Group samples. The authors wish to thank one anonymous reviewer, co-Editor Dr. Kenneth Eriksson and Dr. Nick Butterfield for constructive reviews, which have improved the text. Support came from Exobiology Grant NAG5-3645 and the NASA Astrobiology Institute, the Australian Research Council and Macquarie University, and the Belgian Science Federal Policy Office.

### References

- Allard, B., Templier, J., Largeau, C., 1997. Artfactual origin of mycobacterial bacteran: formation of melanoidin-like artfactual

- Dresselhaus, M.S., Dresselhaus, G., 1982. In: Cardona, M., Guntherodt (Eds.), *Light Scattering in Solids III*. Springer, Berlin, p. 187.
- Escribano, R., Sloan, J.J., Siddique, N., Sze, N., Dudev, T., 2001. Raman spectroscopy of carbon-containing particles. *Vib. Spectrosc.* 26, 179–186.
- Ferrari, A.C., Robertson, J., 2000. Interpretation of Raman spectra of disordered and amorphous carbon. *Phys. Rev. B: Condens. Matter Mater. Phys.* 61, 14095–14107.
- Gelin, F., Volkman, J.K., Largeau, C., Derenne, S., Sinninghe Damste, J.S., De Leeuw, J.W., 1999. Distribution of aliphatic, nonhydrolyzable biopolymers in marine microalgae. *Org. Geochem.* 30, 147–159.
- Goth, K., de Leeuw, J.M., Puttmann, W., Tegelaar, E.W., 1988. Origin of Messel oil shale kerogen. *Nature* 336, 759–761.
- Grey, K., 1998. *Ediacarian acritarchs of Australia*. Ph.D. thesis, Macquarie University.
- Hatcher, P.G., Spiker, E.C., Szeverenyi, N.M., Maciel, G.E., 1983. Selective preservation and origin of petroleum forming aquatic kerogen. *Nature* 305, 498–501.
- Javaux, E.J., Knoll, A.H., Walter, M.R., 2001. Morphological and ecological complexity in early eukaryotic ecosystems. *Nature* 412, 66–69.
- Javaux, E.J., Knoll, A.H., Walter, M.R., 2003. Recognizing and interpreting the fossils of Early Eukaryotes. *Origins Life Evol. Biosphere* 33, 75–94.
- Javaux, E.J., Knoll, A.H., Walter, M.R., 2004a. TEM evidence for eukaryotic diversity in mid-Proterozoic oceans. *Geobiology* 2, 121–132.
- Javaux, E.J., Knoll, A.H., Marshall, C.P., Walter, M.R., 2004b. Recognizing early life on Earth and Mars. *European Space Agency Special Paper*, vol. 545, pp. 127–130.
- Javaux, E.J., Marshall, C.P., submitted. A new approach in deciphering early protist paleobiology and evolution: combined microscopy and microchemistry of single acritarchs.
- Jehlicka, J., Beny, C., Rouzaud, J-N., 1997. Raman microspectrometry of accumulated non-graphitized solid bitumens. *J. Raman Spectrosc.* 28, 717–724.
- Keleman, S.R., Fang, H.L., 2001. Maturity trends in Raman spectra from kerogen and coal. *Energy Fuels* 15, 653–658.
- Kjellstrom, G., 1968. Remarks on the chemistry and ultrastructure of the cell wall of some Palaeozoic leiospheres. *Geol. Foreningens Stockholm Forhandl.* 90, 221–228.
- Knoll, A.H., 1996. *Archaean and Proterozoic palaeontology*. In: Jansonius, J., McGregor, D.C. (Eds.), *Palynology: Principles and Applications*, vol. 1, American Association of Stratigraphic Palynologists Foundation. Publishers Press, Salt Lake City, pp. 51–80, Chapter 4.
- Kokinos, J.P., 1994. *Studies on the cell wall of dinoflagellate resting cysts: morphological development, ultrastructure, and chemical composition*. Ph.D. thesis, Massachusetts Institute of Technology/Woods Hole Oceanographic Institution, Technical Report WHOI-94-10.
- Kokinos, J.P., Eglinton, T.I., Goñi, M.A., Boon, J.J., Martoglio, P.A., Anderson, D.M., 1998. Characterization of a highly resistant biomacromolecular material in the cell wall of a marine dinoflagellate resting cyst. *Org. Geochem.* 28, 265–288.
- Largeau, C., Derenne, S., Casadevall, E., Kadouri, A., Sellier, N., 1986. Pyrolysis of immature Torbanites and of the resistant biopolymer (PRB A) isolated from extant alga *Botryococcus braunii*. Mechanism of formation and structure of Torbanite. *Org. Geochem.* 10, 1023–1032.
- Lin, R., Ritz, G.P., 1993. Studying individual macerals using i.r. microspectroscopy, and implications on oil versus gas/condensate proneness and low rank generation. *Org. Geochem.* 20, 695–706.
- Moldowan, J.M., Talyzina, N.M., 1998. Biogeochemical evidences for dinoflagellate ancestors in the Early Cambrian. *Science* 281, 1168–1170.
- Martin, F., 1993. Acritarchs: a review. *Biol. Rev.* 68, 475–538.
- Nemanich, R.J., Solin, S.A., 1979. First- and second-order Raman scattering from finite-size crystals of graphite. *Phys. Rev. B* 20, 392–401.
- Nikiel, L., Jagodzinski, P.W., 1993. Raman spectroscopic characterization of graphites: a re-evaluation of spectra/structure correlation. *Carbon* 31, 1313–1317.
- Painter, P.C., Snyder, R.W., Starsinic, M., Coleman, M.M., Kuehn, D.W., Davis, A., 1985. Concerning the application of FTIR to the study of coal: a critical assessment of band assignments and the application of spectral analysis programs. *Appl. Spectrosc.* 35, 475–485.



- Talyzina, N.M., Moczydlowska, M., 2000. Morphological and ultrastructural studies of some acritarchs from the Lower Cambrian Lukati Formation, Estonia. *Rev. Palaeobot. Palynol.* 112, 1–21.
- Talyzina, N.M., Moldowan, J.M., Johannisson, A., Fago, F.J., 2000. Affinities of Early Cambrian acritarchs studied by using microscopy, fluorescence flow cytometry and biomarkers. *Rev. Palaeobot. Palynol.* 108, 37–53.
- Tappan, H., 1980. *The Paleobiology of Plant Protists*. Freeman, San Francisco, CA, pp. 148–224.
- Tegelaar, E.W., de Leeuw, J.W., Derenne, S., Largeau, C., 1989. A reappraisal of kerogen formation. *Geochim. Cosmochim. Acta* 53, 3103–3106.
- Traverse, A., 1988. *Paleopalynology*. Unwin Hyman, London, 600 pp.
- Van Waveren, I., 1992. Morphology of probable planktonic crustacean eggs from the Holocene of the Banda Sea (Indonesia). In: Head, M.J., Wrenn, J.H. (Eds.), *Neogene and Quaternary Dinoflagellate Cysts and Acritarchs*. American Association of Stratigraphic Palynologists Foundation, Dallas, pp. 89–120.
- Versteegh, G.J.M., Blokker, P., 2004. Resistant macromolecules of extant and fossil microalgae. *Phycol. Res.* 52, 325–339.
- Vidano, R., Fischbach, D.B., 1978. New lines in the Raman spectra of carbons and graphite. *J. Am. Ceram. Soc.* 61, 13–17.
- Wall, D., 1958. Evidence from recent plankton regarding the biological affinities of *Tasmanites Newton 1875* and *Leiosphaeridia Eisenack*. *Geol. Mag.* 4, 353–362.
- Wynn-Williams, D.D., Edwards, H.G.M., Newton, E.M., Holder, J.M., 2002. Pigmentation as a survival strategy for ancient and